HHS Public Access

Author manuscript

Neuroimage. Author manuscript; available in PMC 2022 December 22.

Published in final edited form as:

Neuroimage. 2022 December 01; 264: 119749. doi:10.1016/j.neuroimage.2022.119749.

Late dominance of the right hemisphere during narrative comprehension

Vahab Youssofzadeh[a,*], **Lisa Conant**[a], **Jeffrey Stout**[a], **Candida Ustine**[a], **Colin Humphries**[a], **William L. Gross**[a,b], **Priyanka Shah-Basak**[a], **Jed Mathis**[a,c], **Elizabeth Awe**[a], **Linda Allen**[a], **Edgar A. DeYoe**[c], **Chad Carlson**[a], **Christopher T. Anderson**[a], **Rama Maganti**[d], **Bruce Hermann**[d], **Veena A. Nair**[e], **Vivek Prabhakaran**[e,f,g], **Beth Meyerand**[e,f,h], **Jeffrey R. Binder**[a], **Manoj Raghavan**[a]

[a]Neurology, Medical College of Wisconsin, Milwaukee, WI, USA

[b]Anesthesiology, Medical College of Wisconsin, Milwaukee, WI, USA

[c]Radiology, Medical College of Wisconsin, Milwaukee, WI, USA

[d]Neurology, University of Wisconsin-Madison, Madison, WI, USA

[e]Radiology, University of Wisconsin-Madison, Madison, WI, USA

[f]Medical Physics, University of Wisconsin-Madison, Madison, WI, USA

[g]Psychiatry, University of Wisconsin-Madison, Madison, WI, USA

[h]Biomedical Engineering, University of Wisconsin-Madison, Madison, WI, USA

Abstract

PET and fMRI studies suggest that auditory narrative comprehension is supported by a bilateral multilobar cortical network. The superior temporal resolution of magnetoencephalography (MEG) makes it an attractive tool to investigate the dynamics of how different neuroanatomic substrates engage during narrative comprehension. Using beta-band power changes as a marker of cortical engagement, we studied MEG responses during an auditory story comprehension task in 31 healthy adults. The protocol consisted of two runs, each interleaving 7 blocks of the story comprehension task with 15 blocks of an auditorily presented math task as a control for phonological processing, working memory, and attention processes. Sources at the cortical surface were estimated with a frequency-resolved beamformer. Beta-band power was estimated in the

*Corresponding author. vyoussofzadeh@mcw.edu (V. Youssofzadeh).

Author contributions

M.R., J.B., W.G., L.C., and C.J.H., designed the experiment. J.S. and C.U. collected the data. V.Y. processed the data and developed the analysis pipeline. V.Y. wrote the manuscript with contributions from M.R., L.C., and J.B. All other authors commented on the paper. M.R. supervised the project.

Declaration of Competing Interest

The authors have declared that no competing interests exist.

Ethics statement

The experimental protocol was approved by the Institutional Review Board (IRB) of the Medical College of Wisconsin (MCW). All participants gave written informed consent, and the approval process of the IRB complies with the declaration of Helsinki.

Supplementary materials

Supplementary material associated with this article can be found, in the online version, at doi:10.1016/j.neuroimage.2022.119749.

frequency range of 16–24 Hz over 1-sec epochs starting from 400 msec after stimulus onset until the end of a story or math problem presentation. These power estimates were compared to 1-second epochs of data before the stimulus block onset. The task-related cortical engagement was inferred from beta-band power decrements. Group-level source activations were statistically compared using non-parametric permutation testing. A story-math contrast of beta-band power changes showed greater bilateral cortical engagement within the fusiform gyrus, inferior and middle temporal gyri, parahippocampal gyrus, and left inferior frontal gyrus (IFG) during story comprehension. A math-story contrast of beta power decrements showed greater bilateral but left-lateralized engagement of the middle frontal gyrus and superior parietal lobule. The evolution of cortical engagement during five temporal windows across the presentation of stories showed significant involvement during the first interval of the narrative of bilateral opercular and insular regions as well as the ventral and lateral temporal cortex, extending more posteriorly on the left and medially on the right. Over time, there continued to be sustained right anterior ventral temporal engagement, with increasing involvement of the right anterior parahippocampal gyrus, STG, MTG, posterior superior temporal sulcus, inferior parietal lobule, frontal operculum, and insula, while left hemisphere engagement decreased. Our findings are consistent with prior imaging studies of narrative comprehension, but in addition, they demonstrate increasing right-lateralized engagement over the course of narratives, suggesting an important role for these right-hemispheric regions in semantic integration as well as social and pragmatic inference processing.

Keywords

Language; Magnetoencephalography; Narrative comprehension; Story; Math; Beta band power decrements

1. Introduction

Narratives, or stories, represent an important element of the human experience from early childhood onward. The comprehension of narratives requires the integration of information across a hierarchy of information processing steps and temporal scales: the brain must access the meanings of individual words (lexical semantics), capture the grammatical relationships between words (syntactic processing), combine word-level meanings to derive the meaning of phrases and sentences, integrate these meanings with existing pragmatic knowledge, and make inferences based on this semantic information (Graesser et al., 1994; Kintsch and van Dijk, 1978; Mar, 2004). The many dimensions of this process require coordination and communication among several brain subsystems, including those involved in working memory, theory-of-mind, and language comprehension (Ferstl et al., 2008; Ferstl and Von Cramon, 2002; Mar, 2011). Spatiotemporal mapping of the relevant brain networks remains a challenge in neuroimaging research.

The neural substrates of auditory narrative comprehension have been shown to involve a bilateral multilobar cortical network that prominently includes the temporal lobe, inferior parietal lobule (IPL), and inferior frontal gyrus (IFG) by many previous functional magnetic resonance imaging (fMRI) studies (AbdulSabur et al., 2014; Awad et al., 2007; Binder et al., 2011; Brennan et al., 2012; Ferstl et al., 2008; Friederici et al., 2000; Lerner et al.,

2011; Mazoyer et al., 1993; Schmithorst et al., 2006; Szaflarski et al., 2012; Vandenberghe et al., 2002). These studies have suggested a bilateral and fairly symmetrical pattern of activations, with some evidence that the right hemisphere is particularly engaged when comprehension requires greater pragmatic inference, such as in interpreting unfamiliar metaphors and distant semantic associations (AbdulSabur et al., 2014; Ferstl et al., 2005; Jung-Beeman, 2005; Lai et al., 2015; Long and Baynes, 2002). Since these aspects of narrative comprehension can only occur after some amount of information has already been integrated from the narrative, one might expect right-hemispheric engagement to increase over the course of a narrative. Increasing right hemisphere involvement was observed by Xu et al. (2005) in an fMRI study using visually presented stories. Specifically, when fMRI activation during the final portion of a written fable was contrasted with that observed during the initial portion of the story, the resulting activation was predominantly seen in the right hemisphere, including regions of lateral and medial prefrontal cortex, anterior middle and inferior temporal gyri, and the angular gyrus.

Given the superior temporal resolution, the dynamics of the underlying processes involved in auditory narrative comprehension can potentially be better resolved by using magnetoencephalography (MEG) (Helenius et al., 2002; Indefrey and Levelt, 2004). MEG can capture the time-frequency dynamics of oscillatory phenomena in the cortex with millisecond resolution (Gross, 2019). Despite this potential advantage, there are far fewer MEG studies of the brain networks engaged in language comprehension compared to alternative modalities such as fMRI (Pylkkänen, 2019). Most M/EEG studies of speech and language comprehension have focused on the processing of phonemes or single words and inferred cortical activations by modeling the sources of event-related fields or potentials (ERFs/ERPs) generated by averaging the time-domain signals following stimulus onset. In contrast to these paradigms, the extraction of meaning from narratives requires the integration of information across sentences. There are several methodological challenges to using ERFs/ERPs to characterize brain responses when stimuli are not impulse-like but extended in time like spoken narratives, and several solutions based on regression or system identification methods have been proposed to deal with them (Brodbeck et al., 2018b; Crosse et al., 2016; de Cheveigné et al., 2018; Lalor et al., 2009; Smith and Kutas, 2015). Extended speech stimuli have been employed in recent years in several MEG studies on aspects of brain function such as frequency domain changes related to the processing of specific types of linguistic components (Armeni et al., 2019), phase and amplitude entrainment of responses in the auditory cortex (Gross et al., 2013), predictive coding (Brodbeck et al., 2022, 2018a; Donhauser and Baillet, 2020; Heilbron et al., 2022; Koskinen et al., 2020), or top-down influences that modulate auditory cortex responses (Park et al., 2020, 2015). The mapping of cortical engagement that can be attributed specifically to the comprehension of narratives was not the focus of these studies. To date, no MEG studies have investigated the slower changes that occur across narratives, resulting from story meaning integration across sentences. It is debatable whether methods based on ERFs/ERPs or regression are suitable for mapping cortical engagement far removed from early sensory areas where assumptions about the linearity of responses may not be valid. Task- or stimulus-related changes in oscillatory power in the cortex provide an alternative to the ERP

framework to map cortical engagement during extended stimuli (Hillebrand et al., 2005; Pfurtscheller, 2001).

A large body of evidence from electrocorticography (ECoG) and M/EEG since the 1980s indicates that an increase in high-frequency power in the gamma band (> 40 Hz), accompanied by a broader field of power decrements in the alpha (8–12 Hz) and beta (13–30 Hz) bands, is the signature of cortical engagement during tasks (Crone et al., 2006, 1998; Eulitz et al., 1996; Miller et al., 2007; Neuper and Pfurtscheller, 2001; Pfurtscheller, 1991; Pfurtscheller and Andrew, 1999; Singh et al., 2002). Several lines of evidence show that high gamma activity is strongly correlated to the firing rates of local neuronal populations (Manning et al., 2009; Nir et al., 2007; Ray and Maunsell, 2011). Both stimulus-related gamma-power increments and beta-power decrements are also strongly correlated to local blood flow and the blood oxygen level-dependent (BOLD) signal (Hall et al., 2014; Muthukumaraswamy and Singh, 2008; Zumer et al., 2010), whereas a similar correspondence between blood flow and ERPs is not always found (Brovelli et al., 2005; Foucher et al., 2003; Logothetis et al., 2001). High gamma-band activity arising outside primary sensory or motor cortices is less readily detectable in M/EEG, very likely due to signal loss caused by the mixing of out-of-phase rhythms at the scalp electrode/MEG sensor (Pfurtscheller and Cooper, 1975) and the presence of a substantial myogenic noise floor at these frequencies (Jerbi et al., 2009; Whitham et al., 2007). However, task-related power decrements in the beta-band have been shown to localize brain areas relevant to language production and/or comprehension by many studies (Armeni et al., 2019; Findlay et al., 2012; Fisher et al., 2008; Hirata et al., 2010, 2004; Kim and Chung, 2008; Youssofzadeh et al., 2020). Our use of beta power decrements as a marker of cortical engagement in this study is guided by these empirical observations and not by any particular theory of cortical oscillations and their role in cognition.

We studied task-related MEG beta power modulations in a group of healthy adults enrolled in the Epilepsy Connectome Project (ECP), who performed a story comprehension task interleaved with a math task during MEG recording. This story-math contrast was originally developed for fMRI to activate areas in the anterior temporal lobe (ATL) that are implicated in conceptual integration and are at risk of damage during temporal lobe epilepsy surgeries (Binder et al., 2011). This task contrast was also implemented for both fMRI and MEG recordings in healthy subjects who were recruited as part of the Human Connectome Project (Larson-Prior et al., 2013; Van Essen et al., 2013). We hypothesized that spatial maps of cortical engagement revealed by task-related beta power decrements during narrative comprehension would be comparable to those observed from fMRI. We further hypothesize that the time course of cortical engagement will reveal progressively greater right-hemispheric engagement as information is accrued over a narrative.

For ease of reporting, we use the term “beta decrements” to refer to decreases in beta-band source power relative to the pre-cue baseline period throughout this paper. In the classical literature, event-related power changes have been referred to as event-related desynchronization (ERD) or event-related synchronization (ERS) depending on the direction of the power change (Neuper et al., 2006; Pfurtscheller and Lopes da Silva, 1999). We

intentionally avoid the terms synchronization and desynchronization because they imply a mechanism for the power change that has yet to be established.

2. Material and methods

2.1. Participants

Our participants were thirty-one adults (13 men and 18 women) who participated in the ECP as healthy controls. The mean age was 31.3 years (SD 8, range 20–55). Participants were native speakers of English, and the majority (27/31, or 87%) were right-handed as determined by the Edinburgh Handedness Inventory (Oldfield, 1971). Written informed consent was obtained from all participants. Participants were paid an hourly stipend. Study procedures were approved by the Institutional Review Board of the Medical College of Wisconsin, Milwaukee, WI, USA.

2.2. Story-math task paradigm

The story-math task paradigm has been described in detail elsewhere (Binder et al., 2011). The version used in the ECP consisted of 2 runs, each with 7 story trials and approximately 14 math trials, as summarized in Fig. 1.

All stimuli were digital audio recordings of natural speech produced by an adult male native speaker of American English. The Story task presented participants with brief spoken stories adapted from Aesop's fables (aesopfables.com), followed by a 2-alternative forced-choice question about the topic of the story. The stories feature social interactions, typically including conversational exchanges, between 2 to 3 human or anthropomorphic (usually animal) protagonists and are designed to illustrate stereotypical human traits and other aphorisms. For example, participants heard, "The rabbits were fighting a war against the eagles and asked the foxes to help them." The foxes replied, "'We would gladly have helped you if we did not know who you were and who you were fighting against.'" See Tables S1–2 for the contents of 14 stories and comprehension questions. The 14 stories ranged from 13.7 to 24.0 seconds in duration, with a mean ± SD duration of 20.3 ± 2.8. Stories contained 3 to 6 sentences (mean = 4.6), 8 to 16 clauses (mean = 10.8), and 39 to 73 words (mean = 60.4). The story task had four levels of difficulty (1 = easiest, 4 = hardest), defined by the vocabulary level and relative similarity of meaning of the response choices. For example, at the easiest level, participants were asked, "That was about foxes or cats?" and at the hardest level, they were asked, "That was about pleasure or assistance?". During the math condition, participants were presented with a series of spoken arithmetic operations, e.g., "fourteen plus twelve equals," with two choices for the response, for example, "twenty-nine or twenty-six". Math problem stimuli ranged from 2 to 13 (6 ± 2.5) seconds in duration. The math problems had 20 available levels of difficulty (1 = easiest, 20 = hardest) defined by the number of operations, size of the integers, and proportion of subtraction operations. In both story and math tasks, the difficulty level was adjusted upward to a harder level whenever the participant accumulated 3 correct responses, whether these were consecutive or not, and adjusted downward to an easier level whenever an error occurred. In theory, this schedule maintains an average accuracy rate of 75% (García-Pérez, 1998). The order

of story presentation across runs was the same for all individuals. We did not conduct any analyses comparing different fables, so no randomization of the order was applied.

Participants responded with their right index and middle finger on a MEG-compatible button pad to select the first or second choice, respectively. They were instructed to respond as accurately as possible while avoiding errors, with a maximum response window of 4 seconds before the start of the next trial. The order of task blocks was counterbalanced between runs. For all participants in the first run, the story task began with trials at difficulty level 3, and the math block began with trials at difficulty level 10. In the second run, the starting difficulty level was set to the level attained at the end of the first run. Each participant completed a total of 7 story questions and 15 math questions during each run of the experiment (i.e., 1 story question and 1 math question per block). Response accuracy (correct trials for the answered questions) and reaction times (time to press the button to indicate a choice relative to the end of the question) were calculated for both the story and math tasks.

In the current study, the math task was specifically selected to isolate the semantic processes involved in narrative comprehension in two primary ways. The first of these was to control for non-semantic processes that were not the focus of the current study. These include not only domain-general attention and executive systems but also auditory and phoneme perception as well as phonological retrieval and working memory (Binder et al., 2011). Second, the use of an attention-demanding, semantically shallow control task is important to suppress activation in areas relevant to semantic processing that otherwise tend to be activated during rest or passive stimulation. In this regard, it is important to note that the resting state is not a neutral state (Buckner et al., 2008; Stark and Squire, 2001). It is an active state during which most people experience vivid and memorable thoughts, images, and emotions. Resting, as well as attentional lapses and task-unrelated thoughts (“mind wandering”) during less demanding tasks, have been associated with activations in regions known as the default mode network (Buckner et al., 2008; Christoff et al., 2009; Mason and Just, 2007). The processes that occur during mind wandering involve the activation and manipulation of acquired knowledge or semantic memory, and studies have shown a significant overlap in regions comprising the default mode network and those involved in semantic tasks (Binder et al., 2009; Huth et al., 2016), including narrative comprehension (Jääskeläinen et al., 2021). Furthermore, there is evidence that the use of a passive or resting control condition can subtract out activation in semantic areas (Binder et al., 2008, 1999; Spitsyna et al., 2006). Thus, we chose to use an attentionally engaging, semantically shallow, verbal task for these analyses to isolate and optimize the examination of the narrative comprehension processes of interest.

2.3. Data acquisition

Participants underwent MEG scanning in the eyes-closed state in an upright position using a 306-channel (204 planar gradiometers and 102 magnetometers) whole-head biomagnetometer system (VectorviewTM, Elekta-Neuromag Ltd., Helsinki, Finland) in a magnetically shielded room (ETS-Lindgren, Eura, Finland) located at Froedtert Hospital, Milwaukee, WI, USA. The MEG data were collected at a sampling rate of 2 kHz using a

high-pass filter with a cutoff frequency of 0.03 Hz. The position of the participant's head relative to the sensors was determined using four head-position indicator coils attached to the scalp surface. Three anatomical landmarks (nasion and left and right pre-auricular points) and the head shape were digitized using a Polhemus Fastrak system (Polhemus; Colchester, VT) for alignment with the anatomical MRI. Task stimuli were presented using E-prime 2.0 Professional (Psychology Software Tools, Inc., Pittsburgh, PA). The audio stimuli were presented at normal listening levels (60 dB above normal hearing levels) via a MEG-compatible headphone (TIP-300, Nicolet Biomedical, Madison, WI). The anatomical MRI of each patient was acquired with a GE Healthcare Discovery MR750 3T MR system. The high-resolution T1 image was acquired with a matrix size of 320×320×230 and a spatial resolution of 0.8×0.8×0.8 mm.

2.4. Data analysis

2.4.1. Preprocessing—A temporal variant of signal space separation using MaxFilter software v2.2 (Elekta-Neuromag, Helsinki, Finland) was applied to remove external magnetic interferences and discard noisy sensors (Taulu and Simola, 2006). The data were downsampled to 1 kHz, segmented into 1-sec epochs, and bandpass filtered (Butterworth with an order of 4) in a frequency range of 1 to 40 Hz. Epochs containing artifacts (SQUID jumps, eye blinks, head movement, or muscles) were removed by thresholding based on a variance exceeding 3×10^{-24} T, kurtosis larger than 15, and z-score larger than 4. Cardiac artifacts were removed using independent component analysis (ICA) based on the infomax algorithm (Bell and Sejnowski, 1995). On average (± SD), 8 ± 4.5 epochs (i.e., seconds) per run were removed across participants.

2.4.2. Beamforming source analysis—MEG data were co-registered to the T1-weighted MR images using common fiducial markers and head shape digitization. To obtain a description of the participant's cortical sheet, cortical surface reconstruction was performed using the Freesurfer image analysis suite (surfer.nmr.mgh.harvard.edu). To reduce the computational demand of source modeling, cortical pial surfaces were downsampled to 15002 vertices. Overlapping spheres were used as a head model to estimate the lead-field matrix required for source modeling.

As described elsewhere (Youssofzadeh et al., 2020), beta source power was estimated using a frequency-resolved spatial filtering beamforming technique called Dynamic Imaging of Coherent Sources, or DICS (Gross et al., 2001). In DICS, the data covariance matrix is used to calculate the spatial filter from the sensor-level cross-spectral densities (CSD), and the filter is applied to the sensor-level CSD to reconstruct the source-level CSDs of pairwise voxel activations. This provides coherence measures between the source pairs (off-diagonal elements of CSD) and source power measures (diagonal elements of CSD). Our analysis only uses the source power estimates.

Sensor-level CSD for each epoch was estimated in the beta frequency range of 16–24 Hz. CSDs were estimated using the Fourier transform and multi-tapering with Discrete Prolate Spheroidal Sequences (Slepian and Pollak, 1961). The center frequency was selected at 20Hz with a spectral smoothing window of 4Hz to have sufficiently smooth spectra and a

zero-padding of 4 seconds to interpolate the baseline and active windows to the same high spectral resolution.

The participant-specific lead fields and CSDs were used to estimate the inverse spatial filters (beamformers) for all the vertices from the combined active and baseline stimulus conditions, implementing the so-called “common filter” approach. Sources were estimated using a lambda regularization parameter *lambda* of 10% (to reduce sensitivity to noise and increase the consistency of the spatial maps across participants) and a fixed dipole orientation (to find sources corresponding to an orientation that maximizes the power). Data from both gradiometers and magnetometers were used for source modeling. To account for the rank deficiency of the covariance matrix due to *MaxFilter*, a truncation parameter of Kappa was set to the singular value decomposition edge discontinuity of combined baseline and active responses (range <=80).

2.4.3. Task contrasts—We analyzed MEG responses occurring during the presentation of the stories and math problems. We did not analyze data from epochs corresponding to the presentation of response choices or the responses themselves. Beta power estimates during the delivery of the story and math problems were compared to power in the pre-stimulus “baseline” periods or against each other. The baseline periods were 1-sec epochs before the onset of the story and math blocks, i.e., inter-block intervals in which no stimulation was being presented, while participants waited for the next story or math block to commence. The MEG responses after narration onset were analyzed over 1-sec epochs (to have equal data length to pre-narration trials) starting from 400 ms post-stimulus onset (to exclude the transient primary sensory cortex responses at stimulus onset) until the end of the story or math problem (see the dashed blue lines in Fig 1). This resulted in an average of 135 epochs (7 trials × 19.3 sec/trial) of the story condition and 80 epochs (15 trials × 5.3 sec/trial) of the math condition per run. The 1-second data segments were selected due to the complexity of the story task and the assumption that semantic processes are usually processed longer than simple word-processing tasks.

To support the choice of beta-band decrement, we investigated the time-frequency representation (TFR) of time-locked responses to story sentences and found strong beta-band decrements for the later activations of the task. A sample baseline corrected TFR from a representative subject completing a story listening task is shown in Fig. Supp. 1.

We first evaluated the group-level beta-power changes during the story and math presentation periods separately by comparing beta-power during Story vs. Baseline and Math vs. Baseline. We then conducted a two-sided paired t-test to obtain Story-vs-Baseline (Story) vs. Math-vs-Baseline (Math) beta power source maps (see Individual and group inferences). Next, we examined the temporal progression of cortical activation during the story comprehension process by contrasting beta-power changes during the five intervals of the narrative separately against all math blocks (i.e., to identify increased beta-power decrements relative to the math task). The goal here was to identify areas that show progressive changes in engagement as information is integrated over the course of the narrative, such as might be expected in brain areas that process pragmatic, social, and affective content. Lastly, to summarize the temporal evolution of hemispheric dominance

during story comprehension, we conducted a laterality analysis using regions that showed cortical engagement during any of the five intervals. The regions were identified from a union of suprathreshold vertices with half-maximum t-values for five intervals (as shown in Fig. 4) and intersected with the Harvard-Oxford atlas ROIs (Kennedy et al., 1998; Makris et al., 1999). A laterality analysis was conducted using the asymmetry index formula LI = (L−R) / (L+R), where L and R are the summed source t-statistics of the left and right hemisphere ROIs, respectively.

2.4.4. Individual and group inferences—At the individual level, beta-band sources were estimated for all data segments of the two task conditions (story and math) and baseline. This resulted in two data matrices of size N×M (N: number of data segments, 80 for math and 135 for stories; and M: number of locations, 15002), For the individual-level analysis, a dependent (paired)-sample t-test was applied separately for each task condition and scan run to statistically quantify the change in mean neural DICS beta source power of the 1-sec task epochs relative to their pre-stimulus baselines. This resulted in one unthresholded t-value map per task, per run, and per participant. The average of the two t-values for each task (one per run) was used as the participant t-map for that task.

For group-level analysis, participant-specific source estimates (unthresholded t-statistics computed in the first-level step) were projected onto a default surface anatomy (MNI-152, nist.mni.mcgill.ca). To identify the group-level significant effects of story and math task responses, two separate one-sample t-tests were conducted against a null hypothesis of zero (Nichols and Holmes, 2002). To compare the story and math conditions directly, a two-sided paired t-test was conducted for the contrast of story and math (story > math and math > story) t-values. Monte Carlo permutation testing was applied with 5000 randomizations, obtaining the maximum statistic across all source locations for each randomization. The signs of the unthresholded t-statistics were randomly flipped across participants in the one-sample t-test, and condition assignment was permuted in the paired t-test analysis. For the two-sided tests, extrema were computed per tail (i.e., two randomization tests, one for the most positive and one for the most negative tests). The maximum statistics control the expected proportion of false positives. A critical alpha value of 0.05 per tail was applied based on this distribution to report significant statistical effects.

To examine beta-power changes in each of the five story intervals, five separate one-sided paired-sample t-tests were conducted comparing each interval against the average of all math block responses. For interpretation purposes, we report the peak MNI coordinates of parceled areas based on the Harvard-Oxford surface atlas.

3. Results

Task performance measures for our participants are summarized in Table 1; data from one participant were lost due to equipment malfunction, and therefore were not included in the behavioral analyses. Reaction times were significantly correlated between the story and math tasks across individual participants ($r = 0.42$, $p < 0.01$, df = 60). Participants completed the story and math tasks with an average accuracy of about 89 percent and 86 percent, respectively. No significant correlation was found between reaction time and

response accuracy for either the story ($r = 0.24$, $p = 0.18$) or the math task ($r = 0.11$, $p = 0.54$).

Brain activity during the presentation of the story and math stimuli revealed robust beta power decreases relative to the baseline periods in widespread regions, with left-hemispheric dominance of the cortical engagement during both tasks, as presented in Fig. 2.

Relative to the pre-stimulus baseline, story presentation resulted in beta power decrements in bilateral temporal regions (inferior temporal gyrus (ITG), MTG, anterior STG, fusiform gyrus, and parahippocampal gyrus), left lateral occipital cortex, bilateral supramarginal gyrus (SMG) and intraparietal sulcus (IPS), bilateral paracentral lobule and mid-cingulate gyrus, bilateral frontoparietal operculum and insula, and left prefrontal cortex, including the IFG, middle frontal gyrus (MFG), and superior frontal gyrus (SFG). Findings for the Math task showed beta power decrements mainly in left-hemispheric regions, including posterior MFG, IFG, posterior STG/SMG, upper central sulcus, and paracentral lobule. Peak MNI coordinates and t-values (with $p < 0.05$) of brain areas engaged in the story and math tasks relative to baseline are reported in Table 2.

The Story-Math contrast showed greater beta power decrements for the former in bilateral regions of the ITG, fusiform gyrus, parahippocampus, cingulate isthmus, and SFG; left MTG; left IFG; left anterior SMG; left paracentral lobule and mid-cingulate gyrus; and right orbital frontal cortex. The contrast showed greater beta power decrements for the math task in left MFG and SFG, right IFG and posterior MFG, bilateral IPS/superior parietal lobule, and left posterior STG/SMG. The t-values (with $p<0.05$) for beta power changes are shown in Fig. 3. The MNI coordinates of the local activation peaks of beta-decrements in different regions are reported in Table 3.

We examined the time course of story-specific brain activation by dividing each story presentation into five equal periods and contrasting each period against the average beta-decrements over the math task. As shown in Fig. 4, the initial period showed cortical engagement in bilateral lateral and ventral temporal regions, with greater posterior temporal and lateral occipital engagement on the left, and greater parahippocampal engagement on the right. There was a bilateral engagement of the central operculum and insula as well as engagement of the left MFG, left dorsal SMG, and right superior parietal lobule. In the second interval, there was a reduced engagement in the left frontal, opercular, anterior temporal, and parietal regions, whereas increasing engagement was seen in the right frontal operculum, insula, medial orbitofrontal cortex, lingual gyrus, and temporal lobe, including the STG, MTG, and anterior parahippocampal gyrus. The third to fifth intervals showed continued cortical engagement in bilateral lateral and ventral temporal regions, particularly anteriorly on the right. There was an increased engagement of the right orbitofrontal cortex, frontal operculum, and insula as well as the right posterior superior temporal sulcus and inferior parietal lobule. Left MFG and SFG engagement, including the dorsomedial prefrontal cortex, is seen in the final phases. The MNI coordinates of the strongest activation regions from the Harvard-Oxford atlas in each period are reported in Table 4.

To visualize these time courses at a regional level, the *t*-value representing the difference in mean beta power decrement during the story task compared to the math was calculated for each parcel in the Harvard-Oxford surface atlas that overlapped with any of the story-math contrast maps, as shown in Fig. 4. Atlas parcels were included if their mean *t*-value was greater than half of the maximum parcel t value for any of the five intervals, and vertices within each of these selected parcels were included for averaging if they exceeded the corrected alpha <.05 threshold used for Fig. 4 during any of the time windows (i.e., if they appeared in the union of the 5 maps in Fig. 4). The included parcels are shown in Fig. 5a.

As summarized in Figs. 5b and 6, the first and second periods showed predominantly bilateral story-specific activation (LIs = −0.01 and −0.02); the third to fifth periods showed increasing right hemispheric dominance, due to both significantly decreased engagement of the left hemisphere and increased right hemisphere engagement (LIs = −0.34, −0.41, and −0.47). Time courses of the individual parcels are shown in Fig. 5c. The laterality of engagement varied across regions during the early phases. In the left hemisphere, temporal and parietal regions generally showed a progressive decrease in activation across the 5 temporal windows. In the right hemisphere, activation in most regions showed a gradual increase in engagement. In the final phase, only a few parcels show left dominance, including the temporooccipital ITG and temporal occipital fusiform cortex. Overall, the findings indicate relative symmetry of engagement during early (first and second intervals of) story processing, a shift to stronger right dominance in temporal and frontal regions, and a shift to very strong right dominance in ventral temporal regions towards the end of the story, i.e., during the middle (third to fifth intervals of) story processing.

4. Discussion

Mapping the time course of cortical engagement during complex cognitive processes is challenging using brain imaging techniques such as PET or fMRI, given their low temporal resolution. By contrast, MEG captures neuromagnetic signals with millisecond resolution, but there are different measures to characterize aspects of neural responses. As is the case for ECoG and EEG signals, there are at least three distinct types of neural responses that can be estimated from neuromagnetic recordings to make inferences about task-related cortical engagement. Historically, the most extensively studied response types in the context of MEG functional imaging are event-related fields, or evoked responses, produced by averaging task-related responses in the time domain. Event-related fields are dominated by low-frequency neural responses that are phase-locked to the stimulus or task-onset and may not be ideally suited to mapping sustained or temporally evolving cortical engagement related to cognitive processes that are extended in time, such as narrative comprehension. Task- or stimulus-related increases in high-gamma (> 70 Hz) power in ECoG or EEG recordings are more directly associated with neuronal firing in the cortex (Crone et al., 2006, 1998; Manning et al., 2009; Miller et al., 2007; Nir et al., 2007; Pfurtscheller, 1991; Ray and Maunsell, 2011) but the detectability of high-gamma activity arising outside primary sensory areas of the cortex in EEG and MEG remains challenging. Task- or stimulus-related power decreases in frequency bands below 35 Hz, which typically accompany high-gamma, provide another marker of cortical engagement that is more easily detected using MEG and has been successfully used for functional imaging (Fisher et al., 2008; Hirata et al.,

2004; Kadis et al., 2008). In this study, we used a source modeling approach based on beta power decrements that we have described previously (Youssofzadeh et al., 2020) to map cortical engagement during the auditory presentation of stories and math problems in a cohort of healthy adults. We show that not only are the story-math contrasts in cortical engagement inferred using this imaging method consistent with fMRI findings for this task (Binder et al., 2011) but that a time-resolved analysis of the responses afforded by MEG reveals progressively greater engagement of the right hemisphere as narratives unfold. The choice of math as a contrast condition was motivated by the need to control for non-semantic processes such as auditory and phonetic perception, attention, and working memory (Binder et al., 2011). The math task also suppresses the mind-wandering and other semantic processes that are active during “resting” and passive states (Binder et al., 2011). Additionally, simple arithmetic processes do not depend on anterior temporal lobe regions (Baldo and Dronkers, 2007; Diesfeldt, 1993). This makes the story-math contrast relevant for studying language comprehension processes, particularly the dynamics of temporal lobe engagement, as a clinical tool in epilepsy surgeries (Binder et al., 2011).

Previous fMRI studies of narrative comprehension have reported relatively symmetric activity in temporal regions (AbdulSabur et al., 2014; Awad et al., 2007; Binder et al., 2009; Fletcher et al., 1995; Gallagher et al., 2000; Schmithorst, 2005; Siebenhühner et al., 2019; Xu et al., 2005; Yarkoni et al., 2008). In our MEG data, consistent with fMRI, beta-power decrements for the story task relative to the math task revealed extensive bilateral temporal engagement. This engagement involved bilateral ventral temporal regions, extending more posteriorly on the left and more anteriorly and medially on the right, including portions of the fusiform gyrus, ITG, and neighboring MTG. These regions are believed to be involved in multimodal integration and concept retrieval (Binder and Desai, 2011; Hickok and Poeppel, 2007, 2004; Ralph et al., 2017; Schuhmann et al., 2012). Over the third to fifth portions of the story, cortical engagement showed increasing right lateralization. While there continued to be significant engagement in left ventrolateral temporal regions, this involvement decreased somewhat in both extent and magnitude over the remainder of the story. In contrast, increases were seen in the engagement of multiple right hemisphere regions, particularly the right temporal pole, STG, inferior parietal region, and frontal cortex. These findings provide novel insights into the temporal dynamics of cortical engagement across broadly distributed right and left hemispheric networks that support narrative comprehension. Interestingly, one previous fMRI study used a visually presented story task with a similar design, dividing fables into early, middle, and final segments (Xu et al., 2005). Consistent with the current study, increasing right hemisphere lateralization was seen across the story such that a contrast of the final segment to the initial segment yielded almost exclusively right hemisphere activation, with greater activation seen in the right anterior MTG/ITG, angular gyrus, frontal operculum, medial prefrontal cortex, and precuneus. The initial portion of the story was contrasted against a passive consonant string viewing condition. There was bilateral but left-lateralized activation for this contrast. The stronger left-lateralization observed by Xu et al. for the initial portion of the story could be due in part to differences in the control task. The contrast in the Xu et al. (2005) study involved a passive, low-level perceptual task that did not control domain-general attention or executive processes, non-semantic (e.g., phonological) language processes, or

potential activation of semantic areas due to task-unrelated thoughts. The presentation modality may also have contributed to the differences as, Spitsyna et al. (2006) reported greater left-lateralized patterns of activation when reading rather than listening to nonfiction passages.

Although patients with acquired unilateral damage to the right hemisphere do not typically show aphasia, multiple studies have suggested that these individuals show significant difficulties with aspects of discourse comprehension, including organizing the elements of a story into a coherent whole (Delis et al., 1983; Wapner et al., 1981), drawing accurate inferences and revising inferences based on new contextual information (Brownell et al., 1986; Silagi et al., 2018), and determining the theme or moral of a story (Hough, 1990; Wapner et al., 1981). Particular comprehension difficulties have been observed when thematic or disambiguating information is presented later in the narrative rather than earlier (Brownell et al., 1986; Hough, 1990), suggesting a particular role of right hemisphere regions in the ongoing integration or updating of interpretations or inferences as new information is presented. In addition, individuals with right hemisphere damage have demonstrated greater difficulties suppressing contextually inappropriate alternative meanings in cases of lexical ambiguity, with this impairment found to be significantly related to narrative comprehension performance (Tompkins et al., 2000). One influential theory proposed to explain right hemisphere involvement in aspects of discourse integration, inferencing, and figurative language interpretation is the fine-coarse semantic coding theory. This theory suggests that, while the left hemisphere shows strong activation of dominant meanings and closely related concepts (i.e., fine coding), the right hemisphere maintains a wider semantic field, weakly activating all meanings and more distantly related concepts (Beeman et al., 1994; Beeman and Chiarello, 1998; Jung-Beeman, 2005). This coarse coding is thought to allow integration across more remotely related concepts as well as revision or reinterpretation if an additional disambiguating context is provided, and could therefore contribute to understanding figurative language, detecting connections across sentences, and deriving themes or generating some types of inferences (Jung-Beeman, 2005). In addition, right hemisphere involvement may be important for suppressing alternative, contextually inappropriate meanings after disambiguation (Tompkins, 2008).

Several neuroimaging studies that investigated the effects of changes in integration difficulty or demands found differential activation in the same right hemisphere regions that showed increasing engagement over the course of the narrative in the current MEG study. For example, previous fMRI (St George et al., 1999) and PET (Nichelli et al., 1995) studies suggested an increased role for the right middle temporal cortex in story comprehension under increased demands for integration, theme detection, or pragmatic inference. In addition, increases in activation in the right anterior MTG, posterior superior temporal sulcus, and inferior parietal lobule were linked with the occurrence of event boundaries in stories, such as changes in location, characters, or goals (Speer et al., 2007). Furthermore, Ferstl and colleagues (Ferstl et al., 2005) observed increased right anterior superior temporal lobe as well as adjacent insular and frontal operculum activation when information inconsistent with global context was introduced to a narrative, which was considered to reflect the increasing difficulty of integration. The right posterior IFG and insula were also reported to be activated in a sentence comprehension paradigm when a polysemous word

was subsequently disambiguated to the subordinate meaning, which was thought to reflect suppression of the initially incorrect interpretation (Mason and Just, 2007). These anterior regions have been implicated in inhibitory control and interference resolution tasks more generally (Bari and Robbins, 2013; Deng et al., 2018).

Importantly, the stories used in the current study were fables and therefore rich in social and affective content with an underlying moral. fMRI studies of theory of mind, which refers to the ability to infer the mental states of others, and emotion processing typically show a bilateral network of frontal, temporal, and parietal regions that largely overlap with the activations seen in story comprehension and in semantic processing tasks more generally (Mar, 2011; Satpute and Lindquist, 2021), including the anterior temporal lobes, posterior superior temporal sulcus, angular gyrus, and dorsomedial prefrontal cortex. While bilateral involvement is indicated by meta-analytic fMRI studies (Mar, 2011; Schurz et al., 2021), clinical studies involving patients with semantic dementia (Irish et al., 2014; Kumfor et al., 2016) have suggested preferential involvement of right anterior temporal regions in aspects of social cognition, such as the theory of mind and emotion recognition. A study of discourse processing in temporal lobe epilepsy (TLE) found both significantly poorer theory of mind and narrative discourse comprehension performance in patients with right TLE relative to those with left TLE (Lomlomdjian et al., 2017). While the theory of mind performance was significantly predictive of narrative discourse comprehension, it did not fully account for the laterality effect on the latter.

Compared to stories, the processing of math problems activated the MFG, mainly on the left side, which has been implicated in many neuroimaging studies concerning math and arithmetic processing (Arsalidou and Taylor, 2011; Dehaene et al., 2004, 1999; Kawashima et al., 2004; Koyama et al., 2017). In one fMRI study, addition and subtraction recruited the left middle frontal cortex, whereas multiplication recruited the left middle and inferior frontal cortices (Kawashima et al., 2004). Math problems also elicited greater involvement of the left anterior superior parietal lobule (SPL), just above the horizontal segment of the intraparietal sulcus (IPS), as well as the right posterior SPL/IPS, both of which have been heavily implicated in numeric cognition and mental arithmetic (Andres et al., 2012; Arsalidou et al., 2018; Arsalidou and Taylor, 2011; Dehaene et al., 2003; Desai et al., 2018; Koenigs et al., 2009; Uddin et al., 2010). Greater beta-band power decrements were also seen in the left posterior STG during the math condition. As demonstrated in patients with strokes (Leff et al., 2009), the posterior STG and SMG are areas associated with phonological retrieval and working memory, which are crucial for math tasks.

One limitation of our study relates to source leakage. Although we employed noise reduction techniques, head modeling based on accurate cortical segmentations, and beamforming source analysis, which mitigate the effects of noise and source leakage, there is a possibility that the deeper cortical sources reported in our study, e.g., fusiform and parahippocampal gyri, are affected by leakage from superficial cortical sources, so caution needs to be exercised when interpreting the activations in these regions. Another possible concern is the use of a prestimulus epoch for baseline correction, given that the neural processes that occur during these “resting” epochs are uncharacterized. Given the extensive evidence that “resting” and other passive states include semantic, episodic memory, and

other complex mental processes, we used these prestimulus epochs only for "baseline correction," which is a standard procedure in MEG and EEG studies. The main contrasts of interest were between the story and math task blocks, which are not affected by the pre-stimulus baseline. Lastly, the number of segments of story and math task epochs in the dataset was unequal, with 135 epochs for the story task and an average of 80 epochs for the math task. We conducted separate group-level source statistics on story and math data segments against their prestimulus baseline and observed source values that met statistical criteria for reliability in all cases. In future research, randomization of narrative and control task blocks, alternative control tasks, longer segments of resting state between blocks, and a balanced number of data segments for the story and control conditions (including resting state) would help facilitate analyses.

Our results demonstrate that source modeling of MEG beta power changes provides a powerful tool for the functional imaging of cognitive processes where induced oscillatory changes may be more suitable markers of cortical engagement than evoked event-related fields. In healthy adults, task-related beta power modulations while listening to stories and solving math problems show differential cortical engagement by the two tasks in ways that are consistent with the fMRI literature on similar tasks and the clinical literature. Progressively greater right hemispheric cortical engagement that we observe during the comprehension of narratives is consistent with what may be predicted based on emerging views on the neuroanatomic substrates of conceptual processing, semantic integration, and social and pragmatic inference processing.

Supplementary Material

Refer to Web version on PubMed Central for supplementary material.

Acknowledgments

This study was supported by grant number U01NS093650 (Epilepsy Connectome Project) from the National Institutes of Health.

Code and data availability

MEG and MRI data were analyzed in MATLAB 2019a (The Mathworks, Inc.) using the FieldTrip v20190419 (fieldtriptoolbox.org) and Brainstorm, v060320 (neuroimage.usc.edu/brainstorm/) toolboxes. Anonymized MEG and structural MRI data, as well as custom code, are available on demand by emailing the corresponding author. A Brainstorm implementation of the DICS beamformer is available at, github.com/vyoussofzadeh/DICS-beamformer-for-Brainstorm.

References

AbdulSabur NY, Xu Y, Liu S, Chow HM, Baxter M, Carson J, Braun AR, 2014. Neural correlates and network connectivity underlying narrative production and comprehension: a combined fMRI and PET study. Cortex 57, 107–127. doi:10.1016/j.cortex.2014.01.017. [PubMed: 24845161]

Andres M, Michaux N, Pesenti M, 2012. Common substrate for mental arithmetic and finger representation in the parietal cortex. Neuroimage 62, 1520–1528. doi:10.1016/j.neuroimage.2012.05.047. [PubMed: 22634854]

Armeni K, Willems RM, van den Bosch A, Schoffelen J-M, 2019. Frequency-specific brain dynamics related to prediction during language comprehension. Neuroimage 198, 283–295. doi:10.1016/j.neuroimage.2019.04.083. [PubMed: 31100432]

Arsalidou M, Pawliw-Levac M, Sadeghi M, Pascual-Leone J, 2018. Brain areas associated with numbers and calculations in children: Meta-analyses of fMRI studies. Dev. Cogn. Neurosci. 30, 239–250. doi:10.1016/j.dcn.2017.08.002. [PubMed: 28844728]

Arsalidou M, Taylor MJ, 2011. Is 2+2=4? Meta-analyses of brain areas needed for numbers and calculations. Neuroimage 54, 2382–2393. doi:10.1016/j.neuroimage.2010.10.009. [PubMed: 20946958]

Awad M, Warren JE, Scott SK, Turkheimer FE, Wise RJS, 2007. A common system for the comprehension and production of narrative speech. J. Neurosci. 27, 11455–11464. doi:10.1523/JNEUROSCI.5257-06.2007. [PubMed: 17959788]

Baldo JV, Dronkers NF, 2007. Neural correlates of arithmetic and language comprehension: a common substrate? Neuropsychologia 45, 229–235. doi:10.1016/j.neuropsychologia.2006.07.014. [PubMed: 16997333]

Bari A, Robbins TW, 2013. Inhibition and impulsivity: behavioral and neural basis of response control. Prog. Neurobiol. 108, 44–79. doi:10.1016/j.pneurobio.2013.06.005. [PubMed: 23856628]

Beeman M, Friedman RB, Grafman J, Perez E, Diamond S, Lindsay MB, 1994. Summation priming and coarse semantic coding in the right hemisphere. J. Cogn. Neurosci. 6, 26–45. doi:10.1162/jocn.1994.6.1.26. [PubMed: 23962328]

Beeman MJ, Chiarello C, 1998. Complementary right- and language comprehension. Curr. Dir. Psychol. Sci. 7, 2–8.

Bell AJ, Sejnowski TJ, 1995. An information-maximization approach to blind separation and blind deconvolution. Neural Comput. 7, 1129–1159. doi:10.1162/neco.1995.7.6.1129. [PubMed: 7584893]

Binder JR, Desai RH, 2011. The neurobiology of semantic memory. Trends Cogn. Sci. 15, 527–536. doi:10.1016/j.tics.2011.10.001. [PubMed: 22001867]

Binder JR, Desai RH, Graves WW, Conant LL, 2009. Where is the semantic system? a critical review and meta-analysis of 120 functional neuroimaging studies. Cereb. Cortex 19, 2767–2796. doi:10.1093/cercor/bhp055. [PubMed: 19329570]

Binder JR, Frost JA, Hammeke TA, Bellgowan PSF, Rao SM, Cox RW, 1999. Conceptual processing during the conscious resting state. A functional MRI study. J. Cogn. Neurosci. 11, 80–93. doi:10.1162/089892999563265. [PubMed: 9950716]

Binder JR, Gross WL, Allendorfer JB, Bonilha L, Chapin J, Edwards JC, Grabowski TJ, Langfitt JT, Loring DW, Lowe MJ, Koenig K, Morgan PS, Ojemann JG, Rorden C, Szaflarski JP, Tivarus ME, Weaver KE, 2011. Mapping anterior temporal lobe language areas with fMRI: a multicenter normative study. Neuroimage 54, 1465–1475. doi:10.1016/j.neuroimage.2010.09.048. [PubMed: 20884358]

Binder JR, Swanson SJ, Hammeke TA, Sabsevitz DS, 2008. A comparison of five fMRI protocols for mapping speech comprehension systems. Epilepsia doi:10.1111/j.1528-1167.2008.01683.x.

Brennan J, Nir Y, Hasson U, Malach R, Heeger DJ, Pylkkänen L, 2012. Syntactic structure building in the anterior temporal lobe during natural story listening. Brain Lang. 120, 163–173. doi:10.1016/j.bandl.2010.04.002. [PubMed: 20472279]

Brodbeck C, Bhattasali S, Cruz Heredia AAL, Resnik P, Simon JZ, Lau E, 2022. Parallel processing in speech perception with local and global representations of linguistic context. Elife 11, 1–28. doi:10.7554/eLife.72056.

Brodbeck C, Hong LE, Simon JZ, 2018a. Rapid transformation from auditory to linguistic representations of continuous speech. Curr. Biol. 28. doi:10.1016/j.cub.2018.10.042, 3976–3983.e5. [PubMed: 30503620]

Brodbeck C, Presacco A, Simon JZ, 2018b. Neural source dynamics of brain responses to continuous stimuli: speech processing from acoustics to comprehension. Neuroimage 172, 162–174. doi:10.1016/J.NEUROIMAGE.2018.01.042. [PubMed: 29366698]

Brovelli A, Lachaux JP, Kahane P, Boussaoud D, 2005. High gamma frequency oscillatory activity dissociates attention from intention in the human premotor cortex. Neuroimage 28, 154–164. doi:10.1016/J.NEUROIMAGE.2005.05.045. [PubMed: 16023374]

Brownell HH, Potter HH, Bihrle AM, Gardner H, 1986. Inference deficits in right brain-damaged patients. Brain Lang. 27, 310–321. doi:10.1016/0093-934X(86)90022-2. [PubMed: 3955344]

Buckner RL, Andrews-Hanna JR, Schacter DL, 2008. The brain's default network: anatomy, function, and relevance to disease. Ann. N. Y. Acad. Sci. 1124, 1–38. doi:10.1196/ANNALS.1440.011. [PubMed: 18400922]

Christoff K, Gordon AM, Smallwood J, Smith R, Schooler JW, 2009. Experience sampling during fMRI reveals default network and executive system contributions to mind wandering. Proc. Natl. Acad. Sci. U. S. A. 106, 8719–8724. doi:10.1073/PNAS.0900234106/SUPPL_FILE/0900234106SI.PDF. [PubMed: 19433790]

Crone NE, Miglioretti DL, Gordon B, Lesser RP, 1998. Functional mapping of human sensorimotor cortex with electrocorticographic spectral analysis II. Event-related synchronization in the gamma band. Brain.

Crone NE, Sinai A, Korzeniewska A, 2006. High-frequency gamma oscillations and human brain mapping with electrocorticography. Prog. Brain Res. doi:10.1016/S0079-6123(06)59019-3.

Crosse MJ, Di Liberto GM, Bednar A, Lalor EC, 2016. The multivariate temporal response function (mTRF) toolbox: a MATLAB toolbox for relating neural signals to continuous stimuli. Front. Hum. Neurosci. 10, 604. doi:10.3389/FNHUM.2016.00604/BIBTEX. [PubMed: 27965557]

de Cheveigné A, Wong DE, Di Liberto GM, Hjortkjær J, Slaney M, Lalor E, 2018. Decoding the auditory brain with canonical component analysis. Neuroimage 172, 206–216. doi:10.1016/J.NEUROIMAGE.2018.01.033. [PubMed: 29378317]

Dehaene S, Molko N, Cohen L, Wilson AJ, 2004. Arithmetic and the brain. Curr. Opin. Neurobiol. 14, 218–224. doi:10.1016/j.conb.2004.03.008. [PubMed: 15082328]

Dehaene S, Piazza M, Pinel P, Cohen L, 2003. Three parietal circuits for number processing. Cogn. Neuropsychol. 20, 487–506. doi:10.1080/02643290244000239. [PubMed: 20957581]

Dehaene S, Spelke E, Pinel P, Stanescu R, Tsivkin S, 1999. Sources of mathematical thinking: behavioral and brain-imaging evidence. Science doi:10.1126/science.284.5416.970, (80-.).

Delis DC, Wapner W, Gardner H, Moses JA, 1983. The contribution of the right hemisphere to the organization of paragraphs. Cortex 19, 43–50. doi:10.1016/S0010-9452(83)80049-5. [PubMed: 6851590]

Deng Y, Wang X, Wang Y, Zhou C, 2018. Neural correlates of interference resolution in the multi-source interference task: a meta-analysis of functional neuroimaging studies. Behav. Brain Funct. 14, 1–9. doi:10.1186/s12993-018-0140-0. [PubMed: 29298719]

Desai RH, Reilly M, Van Dam W, 2018. The multifaceted abstract brain. Philos. Trans. R. Soc. B Biol. Sci. 373, 20170122. doi:10.1098/rstb.2017.0122.

Diesfeldt HFA, 1993. Progressive decline of semantic memory with preservation of number processing and calculation. Behav. Neurol. 6, 239–242. doi:10.3233/BEN-1993-6411. [PubMed: 24487142]

Donhauser PW, Baillet S, 2020. Two distinct neural timescales for predictive speech processing. Neuron 105. doi:10.1016/j.neuron.2019.10.019, 385–393.e9. [PubMed: 31806493]

Eulitz C, Maess B, Pantev C, Friederici AD, Feige B, Elbert T, 1996. Oscillatory neuromagnetic activity induced by language and non-language stimuli. Cogn. Brain Res. 4, 121–132. doi:10.1016/0926-6410(96)00026-2.

Ferstl EC, Neumann J, Bogler C, Von Cramon DY, 2008. The extended language network: a meta-analysis of neuroimaging studies on text comprehension. Hum. Brain Mapp 29, 581–593. doi:10.1002/hbm.20422. [PubMed: 17557297]

Ferstl EC, Rinck M, Von Cramon DY, 2005. Emotional and temporal aspects of situation model processing during text comprehension: an event-related fMRI study. J. Cogn. Neurosci. 17, 724–739. doi:10.1162/0898929053747658. [PubMed: 15904540]

Ferstl EC, Von Cramon DY, 2002. What does the frontomedian cortex contribute to language processing: coherence or theory of mind? Neuroimage 17, 1599–1612. doi:10.1006/nimg.2002.1247. [PubMed: 12414298]

Findlay AM, Ambrose JB, Cahn-Weiner DA, Houde JF, Honma S, Hinkley LBN, Berger MS, Nagarajan SS, Kirsch HE, 2012. Dynamics of hemispheric dominance for language assessed by magnetoencephalographic imaging. Ann. Neurol. 71, 668–686. doi:10.1002/ana.23530. [PubMed: 22522481]

Fisher AE, Furlong PL, Seri S, Adjamian P, Witton C, Baldeweg T, Phillips S, Walsh R, Houghton JM, Thai NJ, 2008. Interhemispheric differences of spectral power in expressive language: a MEG study with clinical applications. Int. J. Psychophysiol. 68, 111–122. doi:10.1016/j.ijpsycho.2007.12.005. [PubMed: 18316134]

Fletcher PC, Happé F, Frith U, Baker SC, Dolan RJ, Frackowiak RSJ, Frith CD, 1995. Other minds in the brain: a functional imaging study of “theory of mind” in story comprehension. Cognition 57, 109–128. doi:10.1016/0010-0277(95)00692-R. [PubMed: 8556839]

Foucher JR, Otzenberger H, Gounot D, 2003. The BOLD response and the gamma oscillations respond differently than evoked potentials: an interleaved EEG-fMRI study. BMC Neurosci. 4, 1–11. doi:10.1186/1471-2202-4-22/FIGURES/3. [PubMed: 12553884]

Friederici AD, Meyer M, Cramon DY, 2000. Auditory language comprehension: an event-related fMRI study on the processing of syntactic and lexical information. Brain Lang. 75, 465–477. doi:10.1006/brln.2000.2438.

Gallagher HL, Happé F, Brunswick N, Fletcher PC, Frith U, Frith CD, 2000. Reading the mind in cartoons and stories: an fMRI study of “theory of mind” in verbal and nonverbal tasks. Neuropsychologia 38, 11–21. doi:10.1016/S0028-3932(99)00053-6. [PubMed: 10617288]

García-Pérez MA, 1998. Forced-choice staircases with fixed step sizes: asymptotic and small-sample properties. Vision Res. 38, 1861–1881. doi:10.1016/S0042-6989(97)00340-4. [PubMed: 9797963]

Graesser AC, Singer M, Trabasso T, 1994. Constructing inferences during narrative text comprehension. Psychol. Rev. 101, 371–395. doi:10.1037/0033-295X.101.3.371. [PubMed: 7938337]

Gross J, 2019. Magnetoencephalography in cognitive neuroscience: a primer. Neuron 104, 189–204. doi:10.1016/j.neuron.2019.07.001. [PubMed: 31647893]

Gross J, Hoogenboom N, Thut G, Schyns P, Panzeri S, Belin P, Garrod S, 2013. Speech rhythms and multiplexed oscillatory sensory coding in the human brain. PLoS Biol. 11, e1001752. doi:10.1371/journal.pbio.1001752. [PubMed: 24391472]

Gross J, Kujala J, Hamalainen M, Timmermann L, Schnitzler A, Salmelin R, 2001. Dynamic imaging of coherent sources: studying neural interactions in the human brain. Proc. Natl. Acad. Sci. U. S. A. 98, 694–699. doi:10.1073/pnas.98.2.694. [PubMed: 11209067]

Hall EL, Robson SE, Morris PG, Brookes MJ, 2014. The relationship between MEG and fMRI. Neuroimage 102 (Pt 1), 80–91. doi:10.1016/J.NEUROIMAGE.2013.11.005. [PubMed: 24239589]

Heilbron M, Armeni K, Schoffelen JM, Hagoort P, De Lange FP, 2022. A hierarchy of linguistic predictions during natural language comprehension. Proc. Natl. Acad. Sci. U. S. A. 119, 1–12. doi:10.1073/pnas.2201968119.

Helenius P, Salmelin R, Service E, Connolly JF, Leinonen S, Lyytinen H, 2002. Cortical activation during spoken-word segmentation in nonreading-impaired and dyslexic adults. J. Neurosci. 22, 2936–2944. doi:10.1523/jneurosci.22-07-02936.2002. [PubMed: 11923458]

Hickok G, Poeppel D, 2007. The cortical organization of speech understanding. Nature 8, 393–402.

Hickok G, Poeppel D, 2004. Dorsal and ventral streams: a framework for understanding aspects of the functional anatomy of language. Cognition doi:10.1016/j.cognition.2003.10.011.

Hillebrand A, Singh KD, Holliday IE, Furlong PL, Barnes GR, 2005. A new approach to neuroimaging with magnetoencephalography. Hum. Brain Mapp. 25, 199–211. doi:10.1002/HBM.20102. [PubMed: 15846771]

Hirata M, Goto T, Barnes G, Umekawa Y, Yanagisawa T, Kato A, Oshino S, Kishima H, Hashimoto N, Saitoh Y, Tani N, Yorifuji S, Yoshimine T, 2010. Language dominance and mapping based on neuromagnetic oscillatory changes: comparison with invasive procedures: clinical article. J. Neurosurg. doi:10.3171/2009.7.JNS09239.

Hirata M, Kato A, Taniguchi M, Saitoh Y, Ninomiya H, Ihara A, Kishima H, Oshino S, Baba T, Yorifuji S, Yoshimine T, 2004. Determination of language dominance with synthetic

aperture magnetometry: comparison with the Wada test. Neuroimage 23, 46–53. doi:10.1016/j.neuroimage.2004.05.009. [PubMed: 15325351]

Hough MS, 1990. Narrative comprehension in adults with right and left hemisphere brain-damage: theme organization. Brain Lang. 38, 253–277. doi:10.1016/0093-934X(90)90114-V. [PubMed: 1691038]

Huth AG, de Heer WA, Griffiths TL, Theunissen FE, Gallant JL, 2016. Natural speech reveals the semantic maps that tile human cerebral cortex. Nature 532, 453–458. doi:10.1038/nature17637. [PubMed: 27121839]

Indefrey P, Levelt WJM, 2004. The spatial and temporal signatures of word production components. Cognition doi:10.1016/j.cognition.2002.06.001.

Irish M, Hodges JR, Piguet O, 2014. Right anterior temporal lobe dysfunction underlies theory of mind impairments in semantic dementia. Brain 137, 1241–1253. doi:10.1093/brain/awu003. [PubMed: 24523434]

Jääskeläinen IP, Sams M, Glerean E, Ahveninen J, 2021. Movies and narratives as naturalistic stimuli in neuroimaging. Neuroimage 224. doi:10.1016/J.NEUROIMAGE.2020.117445.

Jerbi K, Ossandón T, Hamamé CM, Senova S, Dalal SS, Jung J, Minotti L, Bertrand O, Berthoz A, Kahane P, Lachaux JP, 2009. Task-related gamma-band dynamics from an intracerebral perspective: review and implications for surface EEG and MEG. Hum. Brain Mapp. doi:10.1002/hbm.20750.

Jung-Beeman M, 2005. Bilateral brain processes for comprehending natural language. Trends Cogn. Sci. 9, 512–518. doi:10.1016/j.tics.2005.09.009. [PubMed: 16214387]

Kadis D, Smith ML, Mills T, Pang EW, 2008. Expressive language mapping in children using MEG; MEG localization of expressive language cortex in healthy children: application to paediatric clinical populations. Down Syndr. Q. 10, 5–12.

Kawashima R, Taira M, Okita K, Inoue K, Tajima N, Yoshida H, Sasaki T, Sugiura M, Watanabe J, Fukuda H, 2004. A functional MRI study of simple arithmetic - a comparison between children and adults. Cogn. Brain Res. 18, 227–233. doi:10.1016/j.cogbrainres.2003.10.009.

Kennedy DN, Lange N, Makris N, Bates J, Meyer J, Caviness VS, 1998. Gyri of the human neocortex: an MRI-based analysis of volume and variance. Cereb. Cortex 8, 372–384. doi:10.1093/CERCOR/8.4.372. [PubMed: 9651132]

Kim JS, Chung CK, 2008. Language lateralization using MEG beta frequency desynchronization during auditory oddball stimulation with one-syllable words. Neuroimage 42, 1499–1507. doi:10.1016/j.neuroimage.2008.06.001. [PubMed: 18603004]

Kintsch W, van Dijk TA, 1978. Toward a model of text comprehension and production. Psychol. Rev. 85, 363–394. doi:10.1037/0033-295X.85.5.363.

Koenigs M, Barbey AK, Postle BR, Grafman J, 2009. Superior parietal cortex is critical for the manipulation of information in working memory. J. Neurosci. 29, 14980–14986. doi:10.1523/JNEUROSCI.3706-09.2009. [PubMed: 19940193]

Koskinen M, Kurimo M, Gross J, Hyvärinen A, Hari R, 2020. Brain activity reflects the predictability of word sequences in listened continuous speech. Neuroimage 219, 116936. doi:10.1016/J.NEUROIMAGE.2020.116936. [PubMed: 32474080]

Koyama MS, O'Connor D, Shehzad Z, Milham MP, 2017. Differential contributions of the middle frontal gyrus functional connectivity to literacy and numeracy. Sci. Rep. 7, 1–13. doi:10.1038/s41598-017-17702-6. [PubMed: 28127051]

Kumfor F, Landin-Romero R, Devenney E, Hutchings R, Grasso R, Hodges JR, Piguet O, 2016. On the right side? A longitudinal study of left-versus right-lateralized semantic dementia. Brain 139, 986–998. doi:10.1093/brain/awv387. [PubMed: 26811253]

Lai VT, Willems RM, Hagoort P, 2015. Feel between the lines: implied emotion in sentence comprehension. J. Cogn. Neurosci. doi:10.1162/jocn_a_00798.

Lalor EC, Power AJ, Reilly RB, Foxe JJ, 2009. Resolving precise temporal processing properties of the auditory system using continuous stimuli. J. Neurophysiol. 102, 349–359. doi:10.1152/JN.90896.2008. [PubMed: 19439675]

Larson-Prior LJ, Oostenveld R, Della Penna S, Michalareas G, Prior F, Babajani-Feremi A, Schoffelen JM, Marzetti L, de Pasquale F, Di Pompeo F, Stout J, Woolrich M, Luo Q, Bucholz R, Fries

P, Pizzella V, Romani GL, Corbetta M, Snyder AZ, 2013. Adding dynamics to the human connectome project with MEG. Neuroimage 80, 190–201. doi:10.1016/j.neuroimage.2013.05.056. [PubMed: 23702419]

Leff AP, Schofield TM, Crinion JT, Seghier ML, Grogan A, Green DW, Price CJ, 2009. The left superior temporal gyrus is a shared substrate for auditory short-term memory and speech comprehension: evidence from 210 patients with stroke. Brain 132, 3401–3410. doi:10.1093/brain/awp273. [PubMed: 19892765]

Lerner Y, Honey CJ, Silbert LJ, Hasson U, 2011. Topographic mapping of a hierarchy of temporal receptive windows using a narrated story. J. Neurosci. 31, 2906–2915. doi:10.1523/JNEUROSCI.3684-10.2011. [PubMed: 21414912]

Logothetis NK, Pauls J, Augath M, Trinath T, Oeltermann a, 2001. Neurophysiological investigation of the basis of the fMRI signal. Nature 412, 150–157. doi:10.1038/35084005. [PubMed: 11449264]

Lomlomdjian C, Múnera CP, Low DM, Terpiluk V, Solís P, Abusamra V, Kochen S, 2017. The right hemisphere's contribution to discourse processing: a study in temporal lobe epilepsy. Brain Lang. 171, 31–41. doi:10.1016/j.bandl.2017.04.001. [PubMed: 28478355]

Long DL, Baynes K, 2002. Discourse representation in the two cerebral hemispheres. J. Cogn. Neurosci. doi:10.1162/089892902317236867.

Makris N, Meyer JW, Bates JF, Yeterian EH, Kennedy DN, Caviness VS, 1999. MRI-based topographic parcellation of human cerebral white matter and nuclei: II. Rationale and applications with systematics of cerebral connectivity. Neuroimage 9, 18–45. doi:10.1006/nimg.1998.0384. [PubMed: 9918726]

Manning JR, Jacobs J, Fried I, Kahana MJ, 2009. Broadband shifts in local field potential power spectra are correlated with single-neuron spiking in humans. J. Neurosci. 29, 13613–13620. doi:10.1523/JNEUROSCI.2041-09.2009. [PubMed: 19864573]

Mar RA, 2011. The neural bases of social cognition and story comprehension. Annu. Rev. Psychol. 62, 103–134. doi:10.1146/annurev-psych-120709-145406. [PubMed: 21126178]

Mar RA, 2004. The neuropsychology of narrative: story comprehension, story production and their interrelation. Neuropsychologia 42, 1414–1434. doi:10.1016/j.neuropsychologia.2003.12.016. [PubMed: 15193948]

Mason RA, Just MA, 2007. Lexical ambiguity in sentence comprehension. Brain Res. 1146, 115–127. doi:10.1016/j.brainres.2007.02.076. [PubMed: 17433891]

Mazoyer BM, Tzourio N, Frak V, Syrota A, Murayama N, Levrier O, Salamon G, Dehaene S, Cohen L, Mehler J, 1993. The cortical representation of speech. J. Cogn. Neurosci. 5, 467–479. doi:10.1162/jocn.1993.5.4.467. [PubMed: 23964919]

Miller KJ, Leuthardt EC, Schalk G, Rao RPN, Anderson NR, Moran DW, Miller JW, Ojemann JG, 2007. Spectral changes in cortical surface potentials during motor movement. J. Neurosci. 27, 2424–2432. doi:10.1523/JNEUROSCI.3886-06.2007. [PubMed: 17329441]

Muthukumaraswamy SD, Singh KD, 2008. Spatiotemporal frequency tuning of BOLD and gamma band MEG responses compared in primary visual cortex. Neuroimage 40, 1552–1560. doi:10.1016/J.NEUROIMAGE.2008.01.052. [PubMed: 18337125]

Neuper C, Pfurtscheller G, 2001. Evidence for distinct beta resonance frequencies in human EEG related to specific sensorimotor cortical areas. Clin. Neurophysiol. 112, 2084–2097. doi:10.1016/S1388-2457(01)00661-7. [PubMed: 11682347]

Neuper C, Wörtz M, Pfurtscheller G, 2006. ERD/ERS patterns reflecting sensorimotor activation and deactivation. Prog. Brain Res. 159, 211–222. doi:10.1016/S0079-6123(06)59014-4. [PubMed: 17071233]

Nichelli P, Grafman J, Pietrini P, Clark K, Lee KY, Miletich R, 1995. Where the brain appreciates the moral of a story. Neuroreport 6, 2309–2313. doi:10.1097/00001756-199511270-00010. [PubMed: 8747143]

Nichols TE, Holmes AP, 2002. Nonparametric permutation tests for functional neuroimaging: a primer with examples. Hum. Brain Mapp. 15, 1–25. doi:10.1002/hbm.1058. [PubMed: 11747097]

Nir Y, Fisch L, Mukamel R, Gelbard-Sagiv H, Arieli A, Fried I, Malach R, 2007. Coupling between neuronal firing rate, Gamma LFP, and BOLD fMRI is related to interneuronal correlations. Curr. Biol. 17, 1275–1285. doi:10.1016/j.cub.2007.06.066. [PubMed: 17686438]

Oldfield RC, 1971. The assessment and analysis of handedness: the Edinburgh inventory. Neuropsychologia doi:10.1016/0028-3932(71)90067-4.

Park H, Ince RAA, Schyns PG, Thut G, Gross J, 2015. Frontal top-down signals increase coupling of auditory low-frequency oscillations to continuous speech in human listeners. Curr. Biol. 25, 1649–1653. doi:10.1016/J.CUB.2015.04.049. [PubMed: 26028433]

Park H, Thut G, Gross J, 2020. Predictive entrainment of natural speech through two fronto-motor top-down channels. Lang. Cogn. Neurosci. 35, 739. doi:10.1080/23273798.2018.1506589.

Pfurtscheller G, 2001. Functional brain imaging based on ERD/ERS, in: Vision Research. doi:10.1016/S0042-6989(00)00235-2.

Pfurtscheller G, 1991. EEG rhythms - event-related desynchronization and synchronization. pp. 289–296. doi:10.1007/978-3-642-76877-4_20.

Pfurtscheller G, Andrew C, 1999. Event-related changes of band power and coherence: methodology and interpretation. J. Clin. Neurophysiol. doi:10.1097/00004691-199911000-00003.

Pfurtscheller G, Cooper R, 1975. Frequency dependence of the transmission of the EEG from cortex to scalp. Electroencephalogr. Clin. Neurophysiol. 38, 93–96. doi:10.1016/0013-4694(75)90215-1. [PubMed: 45909]

Pfurtscheller G, Lopes da Silva FH, 1999. Event-related EEG/MEG synchronization and desynchronization: basic principles. Clin. Neurophysiol. 110, 1842–1857. [PubMed: 10576479]

Pylkkänen L, 2019. The neural basis of combinatory syntax and semantics. Science 366, 62–66. doi:10.1126/science.aax0050, (80-.). [PubMed: 31604303]

Ralph MAL, Jefferies E, Patterson K, Rogers TT, 2017. The neural and computational bases of semantic cognition. Nat. Rev. Neurosci. 18, 42–55. doi:10.1038/nrn.2016.150. [PubMed: 27881854]

Ray S, Maunsell JHR, 2011. Different origins of gamma rhythm and high-gamma activity in macaque visual cortex. PLoS Biol. 9, 1000610. doi:10.1371/journal.pbio.1000610.

Satpute AB, Lindquist KA, 2021. At the neural intersection between language and emotion. Affect. Sci. 2, 207–220. doi:10.1007/s42761-021-00032-2. [PubMed: 36043170]

Schmithorst VJ, 2005. Separate cortical networks involved in music perception: preliminary functional MRI evidence for modularity of music processing. Neuroimage 25, 444–451. doi:10.1016/j.neuroimage.2004.12.006. [PubMed: 15784423]

Schmithorst VJ, Holland SK, Plante E, 2006. Cognitive modules utilized for narrative comprehension in children: a functional magnetic resonance imaging study. Neuroimage 29, 254–266. doi:10.1016/j.neuroimage.2005.07.020. [PubMed: 16109491]

Schuhmann T, Schiller NO, Goebel R, Sack AT, 2012. Speaking of which: dissecting the neurocognitive network of language production in picture naming. Cereb. Cortex 22, 701–709. doi:10.1093/cercor/bhr155. [PubMed: 21685399]

Schurz M, Radua J, Tholen MG, Maliske L, Margulies DS, Mars RB, Sallet J, Kanske P, 2021. Toward a hierarchical model of social cognition: a neuroimaging meta-analysis and integrative review of empathy and theory of mind. Psychol. Bull. 147, 293–327. doi:10.1037/bul0000303. [PubMed: 33151703]

Siebenhühner F, Wang SH, Arnulfo G, Nobili L, Palva JM, Palva S, 2019. Resting-state cross-frequency coupling networks in human electrophysiological recordings Short title: resting-state cross-frequency coupling networks. doi:10.1101/547638.

Silagi ML, Radanovic M, Conforto AB, Zanotto Mendonça LI, Mansur LL, 2018. Inference comprehension in text reading: performance of individuals with right- versus left-hemisphere lesions and the influence of cognitive functions. PLoS One 13, 1–14. doi:10.1371/journal.pone.0197195.

Singh KD, Barnes GR, Hillebrand A, Forde EME, Williams AL, 2002. Task-related changes in cortical synchronization are spatially coincident with the hemodynamic response. Neuroimage 16, 103–114. doi:10.1006/nimg.2001.1050. [PubMed: 11969322]

Slepian D, Pollak HO, 1961. Prolate spheroidal wave functions, fourier analysis and uncertainty — I. Bell Syst. Tech. J. doi:10.1002/j.1538-7305.1961.tb03976.x.

Smith NJ, Kutas M, 2015. Regression-based estimation of ERP waveforms: I. The rERP framework. Psychophysiology 52, 157–168. doi:10.1111/PSYP.12317. [PubMed: 25141770]

Speer NK, Zacks JM, Reynolds JR, 2007. Human brain activity time-locked to narrative event boundaries: research article. Psychol. Sci. 18, 449–455. doi:10.1111/j.1467-9280.2007.01920.x. [PubMed: 17576286]

Spitsyna G, Warren JE, Scott SK, Turkheimer FE, Wise RJS, 2006. Converging language streams in the human temporal lobe. J. Neurosci. 26, 7328. doi:10.1523/JNEUROSCI.0559-06.2006. [PubMed: 16837579]

St George M, Kutas M, Martinez A, Sereno MI, 1999. Semantic integration in reading: engagement of the right hemisphere during discourse processing. Brain 122, 1317–1325. doi:10.1093/brain/122.7.1317. [PubMed: 10388797]

Stark CEL, Squire LR, 2001. When zero is not zero: the problem of ambiguous baseline conditions in fMRI. Proc. Natl. Acad. Sci. U. S. A. 98, 12760–12765. doi:10.1073/PNAS.221462998/ASSET/D262C189-7C79-4483-BB08-0ADE8CA04AEB/ASSETS/GRAPHIC/PQ2214629003.JPEG. [PubMed: 11592989]

Szaflarski JP, Altaye M, Rajagopal A, Eaton K, Meng XX, Plante E, Holland SK, 2012. A 10-year longitudinal fMRI study of narrative comprehension in children and adolescents. Neuroimage 63, 1188–1195. doi:10.1016/j.neuroimage.2012.08.049. [PubMed: 22951258]

Taulu S, Simola J, 2006. Spatiotemporal signal space separation method for rejecting nearby interference in MEG measurements. Phys. Med. Biol. doi:10.1088/0031-9155/51/7/008.

Tompkins CA, 2008. Theoretical considerations for understanding “understanding” by adults with right hemisphere brain damage. Perspect. Neurophysiol. Neurogenic Speech Lang. Disord. 18, 45–54. doi:10.1044/nnsld18.2.45. [PubMed: 20011667]

Tompkins CA, Baumgaertner A, Lehman MT, Fassbinder W, 2000. Mechanisms of discourse comprehension impairment after right hemisphere brain damage: suppression in lexical ambiguity resolution. J. Speech Lang. Hear. Res. 43, 62–78. [PubMed: 10668653]

Uddin LQ, Supekar K, Amin H, Rykhlevskaia E, Nguyen DA, Greicius MD, Menon V, 2010. Dissociable connectivity within human angular gyrus and intraparietal sulcus: evidence from functional and structural connectivity. Cereb. Cortex 20, 2636–2646. doi:10.1093/cercor/bhq011. [PubMed: 20154013]

Van Essen DC, Smith SM, Barch DM, Behrens TEJ, Yacoub E, Ugurbil K, 2013. The WU-minn human connectome project: an overview. Neuroimage 80, 62–79. doi:10.1016/j.neuroimage.2013.05.041. [PubMed: 23684880]

Vandenberghe R, Nobre AC, Price CJ, 2002. The response of left temporal cortex to sentences. J. Cogn. Neurosci. doi:10.1162/08989290260045800.

Wapner W, Hamby S, Gardner H, 1981. The role of the right hemisphere in the apprehension of complex linguistic materials. Brain Lang. 14, 15–33. doi:10.1016/0093-934X(81)90061-4. [PubMed: 7272721]

Whitham EM, Pope KJ, Fitzgibbon SP, Lewis T, Clark CR, Loveless S, Broberg M, Wallace A, DeLosAngeles D, Lillie P, Hardy A, Fronsko R, Pulbrook A, Willoughby JO, 2007. Scalp electrical recording during paralysis: quantitative evidence that EEG frequencies above 20 Hz are contaminated by EMG. Clin. Neurophysiol. 118, 1877–1888. doi:10.1016/j.clinph.2007.04.027. [PubMed: 17574912]

Xu J, Kemeny S, Park G, Frattali C, Braun A, 2005. Language in context: emergent features of word, sentence, and narrative comprehension. Neuroimage 25, 1002–1015. doi:10.1016/j.neuroimage.2004.12.013. [PubMed: 15809000]

Yarkoni T, Speer NK, Zacks JM, 2008. Neural substrates of narrative comprehension and memory. Neuroimage 41, 1408–1425. doi:10.1016/j.neuroimage.2008.03.062. [PubMed: 18499478]

Youssofzadeh V, Stout J, Ustine C, Gross WL, Conant LL, Humphries CJ, Binder JR, Raghavan M, Lisa L, Humphries CJ, Binder JR, Raghavan M, 2020. Mapping language from MEG beta power modulations during auditory and visual naming. Neuroimage doi:10.1016/j.neuroimage.2020.117090.

Zumer JM, Brookes MJ, Stevenson CM, Francis ST, Morris PG, 2010. Relating BOLD fMRI and neural oscillations through convolution and optimal linear weighting. Neuroimage 49, 1479–1489. doi:10.1016/J.NEUROIMAGE.2009.09.020. [PubMed: 19778617]

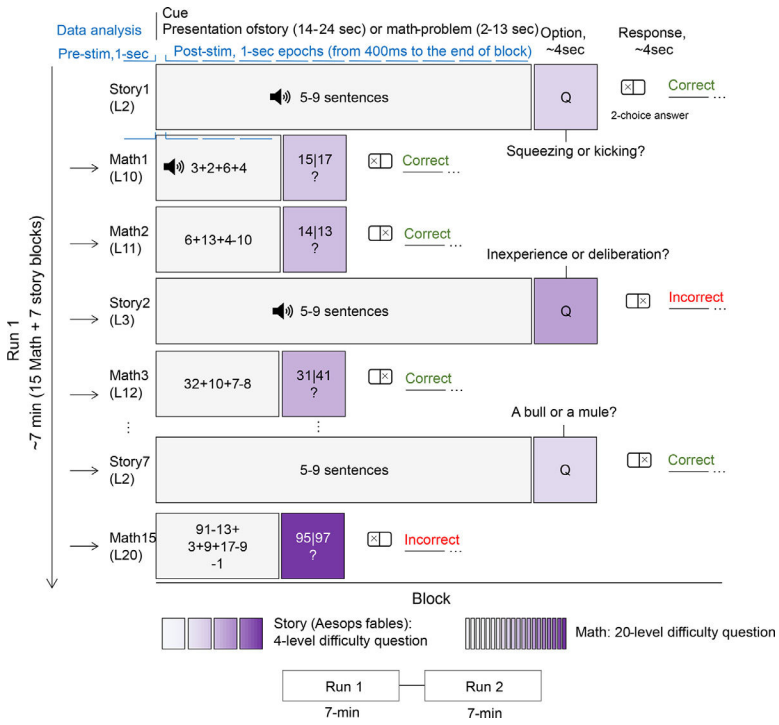

Figure 1.

The Story-Math task. The story-math task consists of two runs, each interleaving 7 blocks of the story and 15 blocks of the math tasks, with an average block duration of 14–24 and 2–13 seconds for story and math blocks, respectively. The story blocks present participants with brief auditory stories (5–9 sentences) adapted from Aesop's fables (www.aesopfables.com), followed by a 2-alternative forced-choice question that asks participants about the topic of the story. The math task consisted of auditorily presenting addition and subtraction problems that the subjects responded to. Task difficulty was adjusted to maintain a response accuracy of ~ 75%.

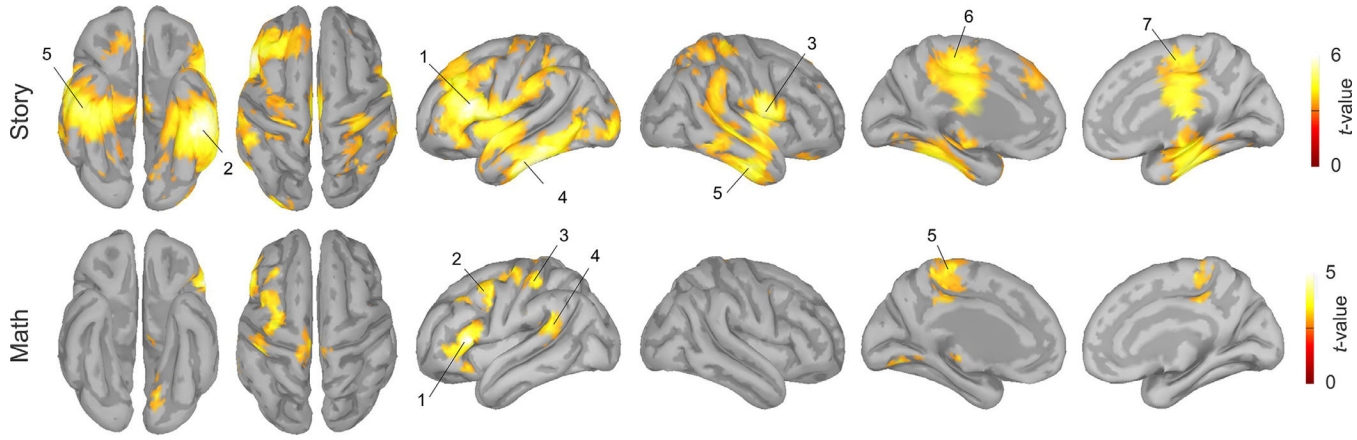

Figure 2.

Beta-power decrements relative to baseline during story and math-problem presentation. The maps represent the *t*-values for the beta decrement of the story (first row) and math conditions (second row) identified by the DICS beamformer source analysis. The *t*-values were obtained from a one-sample t-test of beta-band relative source powers against a null hypothesis. Source activations (*t*-values for beta-power decrements) with pFWE < 0.05 are displayed on an inflated template (MNI-152) with dark representing sulci and gray representing gyri. The *t*-values and MNI coordinates of the local activation peaks in specific areas are reported in Table 2. T-values greater than 4.3 and 3.4 are shown for the story and math task responses, respectively.

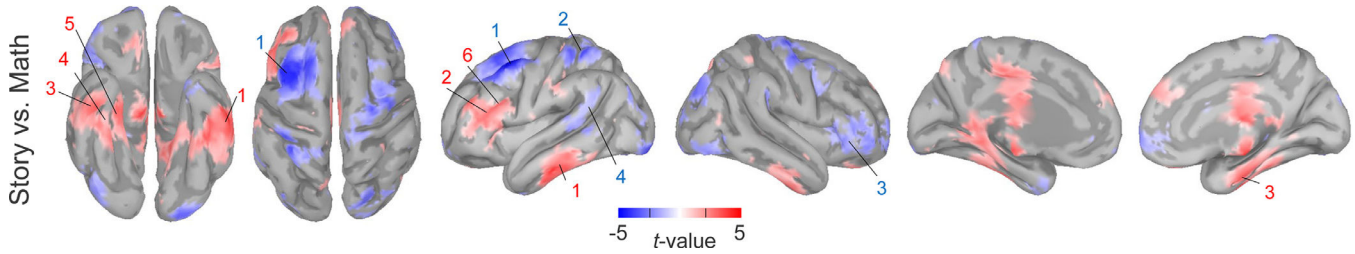

Figure 3.

Comparison between story and math beta power decrements. Areas, where Story-beta-decrements > Math-beta-decrements (red) and Math-beta-decrements > Story-beta-decrements (blue) based on a two-sided paired t-test of beta power changes are displayed using a diverging color scale. T-values greater than absolute 3.5 are shown. Corresponding *t*-values and MNI coordinates of activation peaks within the numbered regions are reported in Table 3.

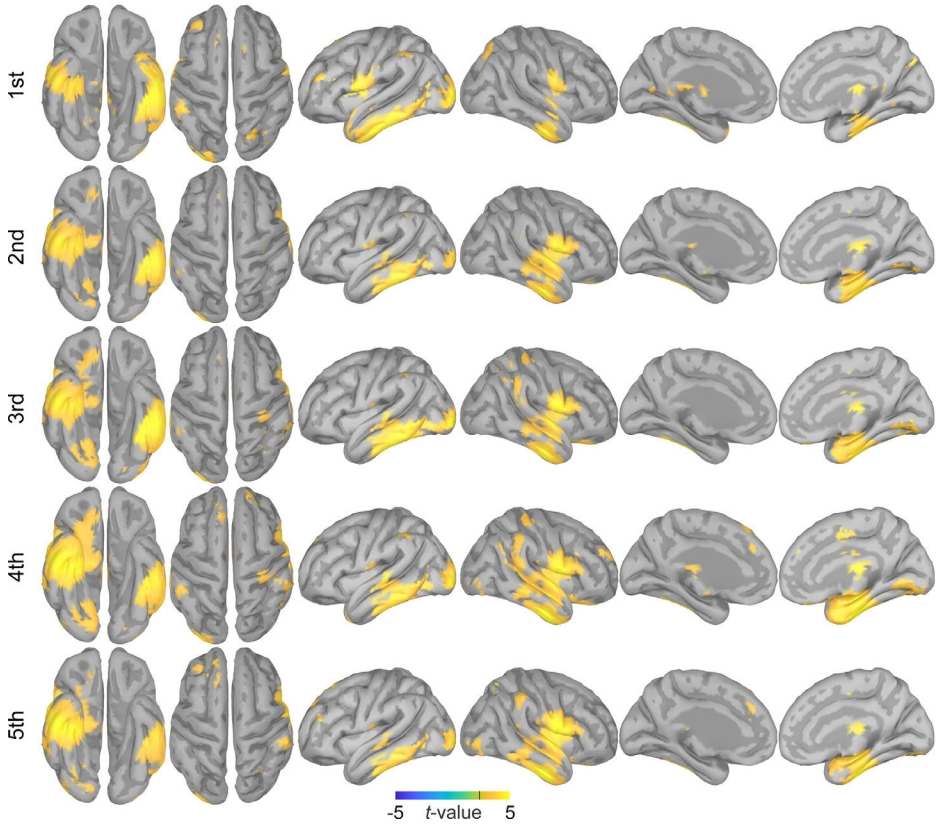

Figure 4.

Cortical engagement for five temporal windows defined over the story presentation, relative to the math problem presentation periods. The cortical maps represent beta power decrements for five intervals of the first, second, third, fourth, and fifth temporal windows of the story presentation condition relative to the math condition. Corresponding t-values and MNI coordinates of the local activation peaks are reported in Table 4. The contrasting condition, math blocks, is shown in Fig. 2. All five story intervals were contrasted against the same time-averaged math response shown in Fig. 2.

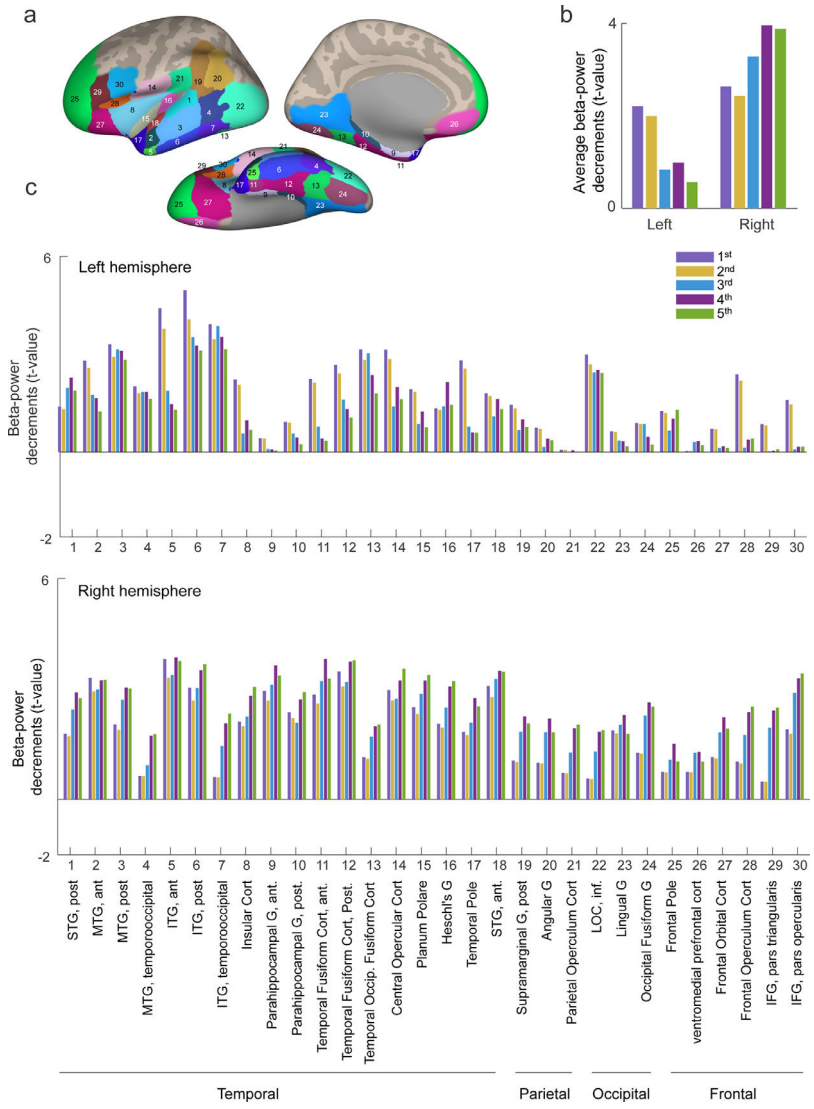

Figure 5.

Beta-power decrements of regions significantly engaged in any of the five intervals of story comprehension relative to math. (a) Regions were identified from a union of suprathreshold engagement with a half-maximum t-value of the corresponding source maps and intersected with the Harvard-Oxford atlas ROIs. A total of 60 (30×2) cortical parcels from the Harvard-Oxford atlas were identified. The selected regions were 1. STG, post, 2. MTG, ant, 3. MTG, post, 4. Temporal-occipital MTG, 5. ITG, ant, 6. ITG, post, 7. Temporal-occipital ITG, 8. Insula., 9. parahippocampal g, ant, 10. Parahippocampal g, post, 11. Temporal fusiform g, ant, 12. Temporal fusiform g, post, 13. Temporal-occipital fusiform g, 14. Central opercular cortex, 15. Planum polare, 16. Heschl's g, 17. Temporal pole, 18. STG, ant, 19. Supramarginal g, 20. Angular g, 21. Parietal operculum, 22. LOC, 23. Lingual g, 24. Occipital fusiform g, 25. Frontal pole, 26. Ventromedial prefrontal cortex, 27. Frontal orbital cortex, 28. Frontal opercular cortex, 29. IFG pars triangularis, 30. IFG pars opercularis. (b). Beta power decrements are summarized in the left and right hemispheres (c) and 30 selected regions.

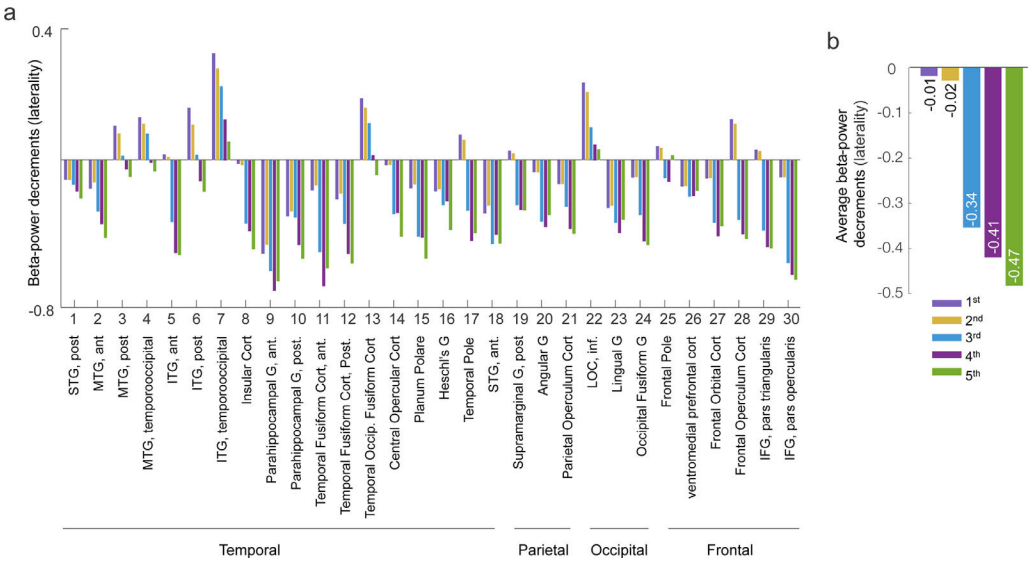

Figure 6.

Laterality indices of regions involved in the five selected time intervals of story comprehension relative to math. (a) Beta-power-decrement laterality indices are summarized in 30 selected regions and (b) the whole cortex. Laterality analysis was conducted on the selected regions shown in Fig. 5A. The negative and positive asymmetry index values represent right and left hemispheric dominance, respectively.

Table 1

Task performance measures during the story-math MEG tasks.

30 healthy controls, 12 men, 18 women		
Behavioral	**Story**	**Math**
Response time (sec.)	0.68 ± 0.26	0.56 ± 0.32
Task accuracy (%)	89.53 ± 6.96	86.55 ± 7.66
Task difficulty level (Story: 1–4 and Math: 1–20)	3.13 ± 0.30	11.85 ± 1.72

Table 2

Cortical regions engaged by the story and math tasks based on beta-power decrements relative to baseline. MNI peak coordinates of beta-power decrements are provided. R and L indicate right and left hemispheric regions. ROI labels are based on the Harvard-Oxford cortical atlas.

Story task, one-sample t-test, beta-power decrements against the pre-stimulus baseline				
#	**Region (Label)**	**Hemisphere (left/right)**	***t*-value (*p*)**	**Coordinate MNI (x, y, z)**
1	Inferior frontal G, tri	L	5.35 (0.002)	−56 27 23
2	Inferior temporal G, mid	L	5.29 (0.002)	−45 −34 −19
3	Rolandic operculum	R	4.72 (0.013)	55 −1 11
4	Inferior temporal G, ant	L	4.7 (0.014)	−63 −14 −33
5	Inferior temporal G, ant	R	4.47 (0.027)	47 −16 −39
6	Cingulate G	L	4.36 (0.037)	−11 −18 46
7	Cingulate G	R	4.31 (0.042)	1.2 −14 37
Math task				
1	Inferior frontal G, tri	L	5.12 (0.002)	−57 20 9
2	Precentral G	L	3.87 (0.01)	−39 7 45
3	Postcentral G	L	3.71 (0.02)	−51 −36 58
4	Superior temporal G	L	3.51 (0.03)	−67 −46 23
5	Paracentral lobule	R	3.48 (0.04)	−1 −28 71

Table 3

Regions involved in story-vs-math task conditions. MNI peak coordinates of beta-power source values are provided. R and L indicate right and left hemispheric regions. ROI labels are based on the Harvard-Oxford cortical atlas.

Story > Math, two-sided paired t-test, beta-power decrements				
#	**Region (Label)**	**Hemisphere (left/right)**	***t*-value (*p*)**	**Coordinate MNI (x, y, z)**
1	Inferior temporal G, post	L	4.68 (0.001)	−52 −27 −29
2	Inferior frontal G, pars triangularis	L	4.25 (0.005)	−43, 36, 11
3	Inferior temporal G, post	R	3.90 (0.013)	55 −16 −39
4	Parahippocampal G, ant	R	3.83 (0.015)	27 −15 −34
5	Temporal fusiform cort, post	R	3.77 (0.018)	24 −4.5 −39
6	Inferior frontal G, pars opercularis	L	3.71 (0.021)	−54 23 24
Story < Math				
1	Middle frontal G	L	−4.17 (0.006)	−41 18 55
2	Superior parietal lobule	L	−3.80 (0.017)	−44 −50 62
3	Inferior frontal G, pars triangularis	R	−3.74 (0.02)	59 28 9.2
4	Superior temporal G	L	−3.57 (0.03)	−68 −49 13

Table 4

Cortical regions engaged during the 5 temporal windows defined for the story comprehension task. Regions are reported for 5 temporal windows during the story presentation period contrasted against the entirety of the math-task presentation period. MNI peak coordinates of beta-power source values are provided. R and L specify the right and left hemispheric regions. ROIs labels are based on the Harvard-Oxford cortical atlas.

1st interval, Story vs. Math, beta-power decrements				
#	**Region (Label)**	**Hemisphere (left/right)**	***t*-value (*p*)**	**Coordinate MNI (x, y, z)**
1	Inferior temporal G., post	L	5.33 (0.001)	−52. −27, −29
2	Inferior temporal G., ant.	L	4.74 (0.001)	−46, 1, −40
3	Inferior temporal G., ant	R	4.55 (0.004)	52, 0, −42
4	Inferior temporal G, temporooccipital	L	4.22 (0.01)	−56, −50, −28
5	Temporal fusiform cort., post.	R	4.15 (0.01)	52, −60, −24
6	Middle temporal G., ant	R	3.95 (0.01)	60, 0, −16
2nd interval				
1	Inferior temporal G, post	L	5.8 (0.001)	−52. −28, −28
2	Inferior temporal G, ant	L	4.4 (0.004)	−46, 1, −40
3	Inferior temporal G, ant	R	5.27 (0.008)	52, 1, −42
4	Inferior temporal G, temporooccipital	L	4.96 (0.01)	−56, −50, −28
5	Temporal fusiform Cort, post	R	4.88 (0.01)	33, −20, −32
6	Middle Temporal G, ant	R	4.66 (0.01)	60, 0, −16
3rd interval				
1	Inferior temporal G, temporooccipital	L	4.73 (0.004)	−56, −50, −28
2	Inferior temporal G, ant	R	4.66 (0.008)	52, 0, −42
3	Superior temporal G, ant	R	4.14 (0.01)	64, 0, 8
4	Temporal fusiform Cor, ant	R	4.06 (0.01)	24, −4, −52
5	Temporal fusiform Cortex, post	R	3.86 (0.01)	32, −20, −32
6	Inferior temporal G, post	L	3.81 (0.01)	−52, −28, −28
4th interval				
1	Inferior temporal G, ant	R	4.87 (0.007)	52, 0, −42
2	Temporal fusiform Cortex, ant	R	4.84 (0.008)	52, −60, −24
3	Temporal fusiform Cortex, post	R	4.79 (0.009)	32, −20, −32

1st interval, Story vs. Math, beta-power decrements				
#	Region (Label)	Hemisphere (left/right)	t-value (p)	Coordinate MNI (x, y, z)
4	Parahippocampal G, ant	R	4.68 (0.009)	24, −4, −40
5	Inferior temporal G, post	R	4.53 (0.009)	52. −28, −28
6	Superior temporal G, ant	R	4.43 (0.01)	64, 0, −8
5th interval				
1	Temporal fusiform Cortex, post	R	4.86 (0.007)	32, −20, −32
2	Inferior temporal G, ant	R	4.84 (0.009)	46, 0, −40
3	Inferior temporal G, post	R	4.74 (0.01)	52. −28, −28
4	Central opercular Cortex	R	4.71 (0.01)	64, −8, 8
5	Superior temporal G, ant.	R	4.50 (0.01)	64, 0, −8
6	Inferior frontal G, pars opercularis	R	4.48 (0.01)	60, 16, 16